Mechanistic Modeling of Stress-Induced Glucose Dysregulation: Calibrating a Coupled HPA-Metabolic Framework to the UK Biobank

Rezo Getsadze[1 [0009−0008−1153−2455]], Qiziyi Cao[1 [0009−0006−8394−0277]], Shivam Kumar[2 [0009−0005−6766−6565]], and Vivek M. Sheraton[2 [0000−0002−6577−6016]]

[1] University of Amsterdam, Amsterdam, Netherlands
[2] Computational Science Lab, University of Amsterdam, Amsterdam, Netherlands
rezi@nyu.edu, ziyi.cao@student.uva.nl, s.kumar@uva.nl, v.s.muniraj@uva.nl

Abstract. Type 2 Diabetes (T2D) is a heterogeneous metabolic disorder driven by the interplay between endocrine stress and glucose regulation. We adapt an 18-variable ordinary differential equation (ODE) model of the hypothalamic-pituitary-adrenal (HPA) and metabolic systems to a UK Biobank pilot cohort ($N = 100$) representing metabolic extremes (50 healthy, 50 T2D). Scaling mechanistic models is challenged by inherent population metabolic diversity. To address this, we implement an individualized scaling framework anchoring glucose uptake and hepatic production to baseline fasting glucose. Results demonstrate that this approach reproduces clinical bimodal distributions and phenotypic attractors without manual refitting. Validation against independently observed HbA1c ($r = 0.82$, $p < 0.0001$, $n = 95$) confirms that the simulated steady states track a clinically meaningful glycemic marker not used during model initialization. By achieving statistical parity using only baseline glucose and mental health data, this framework enables scaling neuroendocrine-metabolic models to the full UK Biobank for virtual trials and personalized interventions.

Keywords: Mechanistic Modeling · HPA Axis · Type 2 Diabetes · UK Biobank · Individualized Calibration.

1 Introduction

The relationship between psychosocial stress and Type 2 Diabetes (T2D) has transitioned from a noted clinical correlation to an established driver of the chronic hyperglycemia and insulin resistance that define the disease. Although traditional risk factors, like diet and physical activity, are well-documented, longitudinal evidence increasingly identifies psychosocial burden and depressive symptoms as potent and independent contributors to cardiometabolic risk [11]. Most compellingly, data from the Whitehall II study identified that alterations in the diurnal cortisol rhythm, specifically raised evening cortisol and a flattened diurnal slope, serve as independent predictors of new-onset T2D over a ten-year

ICCS Camera Ready Version 2026
To cite this paper please use the final published version:
DOI: 10.1007/978-3-032-29912-3_33

period [15]. Despite these clinical associations, the long-term physiological pathways through which stress burden manifests as metabolic dysfunction remain difficult to quantify at a population scale [26].

This cumulative physiological "wear and tear," often termed allostatic load, drives a gradual deterioration in glucose regulation known as "metabolic drift" [8]. Quantitative evidence from the Multi-Ethnic Study of Atherosclerosis (MESA) has further characterized this drift, showing that every 1% flatter overall cortisol decline slope is associated with a 0.19% subsequent annual increase in fasting glucose among individuals with diabetes [10].

Cao et al. [6] proposed a mechanistic framework to address this by coupling the hypothalamic-pituitary-adrenal (HPA) axis with the glucose-insulin metabolic loop. This system, based on the stress-diabetes interplay framework established by Bumbuc and Sheraton [5], maps stress burden to a sustained endocrine drive that propagates through the regulatory chain of CRH, ACTH, and Cortisol. Cortisol acts as the primary mediator, influencing both hepatic glucose production (HGP) and peripheral insulin sensitivity (S_i). Mechanistically, glucocorticoids induce a post-receptor defect of insulin action, shifting the insulin dose-response curve for both HGP suppression and peripheral utilization [27]. Furthermore, elevated cortisol has been shown to increase total glucose production by approximately 18%, an effect driven primarily by upregulated gluconeogenic flux [22].

We apply this coupled HPA-metabolic model to a "twin" pilot cohort from the UK Biobank (UKB) [29]. By focusing on the metabolic extremes (50 healthy controls and 50 Type 2 Diabetics), the model's ability to maintain distinct phenotypic attractors is evaluated. Unlike traditional mechanistic models that rely on phenotype-specific parameter sets, we implement an individualized scaling approach where liver production and insulin sensitivity are anchored to each participant's baseline glucose. We hypothesize that this coupled framework can replicate the clinical bimodal glucose distributions observed in the UK Biobank without requiring group-level manual refitting. We investigate whether the model can maintain mathematical stability and reproduce population-level statistics while capturing the divergent metabolic resilience observed under sustained psychosocial stress.

2 Methods

The Coupled ODE Framework The computational framework consists of 18 coupled ordinary differential equations (ODEs) representing the interaction between the hypothalamic-pituitary-adrenal (HPA) axis and glucose-insulin metabolic dynamics (see Appendix A for the modified equations; the complete system is defined in Cao et al. [6]). This system, based on the architecture proposed by Cao et al. [6], allows for the simulation of long-term metabolic drift in response to sustained psychosocial stress. While the ODE architecture is inherited from Cao et al., the present work makes three substantive modifications: (1) the stress drive is derived from UK Biobank Mental Health Questionnaire fields rather than

ICCS Camera Ready Version 2026
To cite this paper please use the final published version:
DOI: 10.1007/978-3-032-29912-3_33

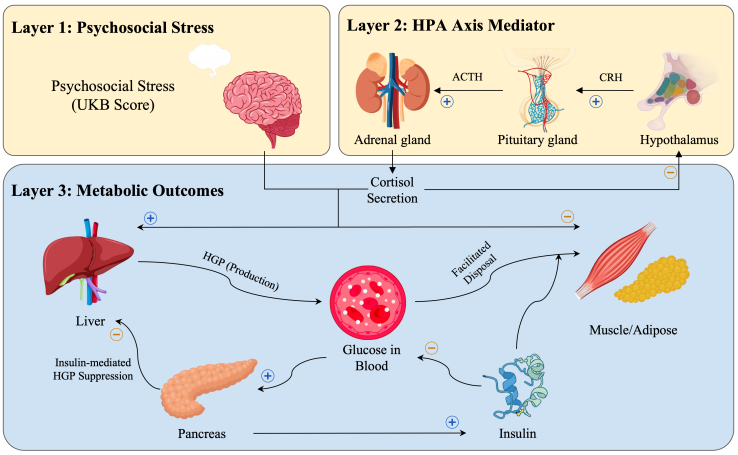

Fig. 1: Mechanistic architecture of the coupled HPA-metabolic system. Psychosocial stress drive (u_{inp}) propagates through the endocrine signaling chain to regulate the metabolic steady state via hepatic production and peripheral sensitivity.

validated clinical depression scores; (2) population-wide constants for glucose uptake (E) and hepatic production (H_{bas}) are replaced with individualized per-patient values anchored to baseline fasting glucose; and (3) a cortisol coupling floor ($\rho = 0.08$) and an uptake floor ($\phi = 0.75 \cdot E_{ref}$) are introduced to ensure numerical stability across the full glycemic range of the UK Biobank cohort. Cao et al. operated on population-averaged parameters fitted to the MESA cohort; the individualized scaling framework described below is this paper's primary methodological contribution.

The system is structured into three layers, illustrated in Figure 1. Psychosocial stress burden, quantified from the UK Biobank Mental Health Questionnaire, serves as the external drive u_{inp} (Layer 1). This drive stimulates the hypothalamus, initiating the CRH-ACTH-Cortisol signalling chain of the HPA axis (Layer 2) [8]. Cortisol then propagates into the metabolic module (Layer 3), where it modulates two key parameters: hepatic glucose production (HGP) and peripheral insulin sensitivity (S_i), governing the interplay between the liver, pancreas, and muscle/adipose tissue. Glucose dynamics are governed by the balance between hepatic production (H) and peripheral disposal (R), where H increases with cortisol, while R is suppressed via insulin inhibition:

$$\frac{dG}{dt} = H(C, G) - R(C, G, I) \tag{1}$$

The state vector y includes 18 variables, accounting for physiological markers such as inflammatory cytokines and BMI. This dimensionality is necessary to model the gradual metabolic drift toward T2D within the UKB cohort [5].

Data Acquisition and Preprocessing Data were obtained from the UK Biobank [29]. This pilot study utilizes a balanced cohort of 50 healthy and 50 T2D par-

ICCS Camera Ready Version 2026
To cite this paper please use the final published version:
DOI: 10.1007/978-3-032-29912-3_33

ticipants to test the scaling logic on metabolic extremes. As this constitutes a mechanistic calibration rather than a predictive study, no train-test split was applied; all 100 participants were used to verify parameter stability and distributional parity. Biometric fields including height (Field 50), weight (Field 21002), and BMI (Field 21001) were used for model configuration, with blood glucose (Field 30740) serving as the primary metabolic anchor for each participant.

The healthy cohort was filtered by requiring the absence of any diabetes diagnosis across all available recruitment instances (Field 2443) and the absence of gestational diabetes history (Field 4041) at any instance, using an IS NOT Yes criterion to avoid excluding participants with missing follow-up data. The diabetic cohort included individuals with a confirmed diagnosis at Instance 0, with gestational-only cases excluded via the same criterion. Participants with missing values in core biomarker or psychosocial fields were excluded to ensure a complete initialization of the 18-variable state vector; medication fields (Field 20003, Arrays 0-7) were treated as sparse by design and filled with zero prior to exclusion, as empty slots indicate no medication rather than missing data. Participants receiving glucose-lowering medications (metformin or insulin) at Instance 0 or Instance 1 were additionally excluded to isolate untreated disease trajectories.

To quantify the psychosocial stress drive (S), we utilized $N = 16$ self-report items from the UKB Mental Health Questionnaire (Fields 20505 to 20520). These items assess the frequency of symptoms such as depressed mood, anxiety, and restlessness over the preceding two weeks. Because these fields are coded on a frequency scale of 1-4 in the UK Biobank, we applied the following transformation to derive a normalized score:

$$S = \frac{\sum_{i=1}^{N}(F_i - \kappa)}{\Omega} \tag{2}$$

where F_i represents the score of the i-th field, $N = 16$ is the number of items, $\kappa = 1$ is the scoring offset, and $\Omega = 48$ is the normalization constant corresponding to the maximum aggregate score across the items. The resulting value $S \in [0, 1]$ represents each individual's normalized stress burden. The linear summation of items was selected over validated composite scales (e.g., PHQ-9) for three pragmatic reasons: the 16 UKB fields collectively span depressive, anxious, and somatic symptom domains that no single existing instrument covers simultaneously; the resulting composite exhibits adequate internal consistency within the UKB cohort [5]; and the transformation preserves monotonicity with respect to clinical severity, which is the property required to drive the ODE stress parameter u within its physiological bounds. Principal component analysis was evaluated as an alternative but discarded as it produces latent scores without direct physiological interpretability. This was then mapped to the model's psychological drive parameter (u), ensuring the HPA axis operates within its physiological range:

$$u = u_{min} + (S \cdot \Delta u) \tag{3}$$

ICCS Camera Ready Version 2026
To cite this paper please use the final published version:
DOI: 10.1007/978-3-032-29912-3_33

where $u_{min} = 18.7$ represents the minimum drive required to uphold endocrine system processes and $\Delta u = 6.3$ is the scaling factor required to reach the model's upper stress threshold. The linear shift ensures that individuals with a minimum stress score maintain the basal drive necessary for physiological signaling, while the maximum score reaches the upper boundary of the simulated HPA activation.

Numerical Stability and Calibration Initial UK Biobank simulations revealed numerical instability in the glucose disposal rate (R) under the high endocrine drive characteristic of chronic stress. To maintain deterministic integrity, we refined the cortisol coupling coefficient to $\rho = 0.08$, which governs the rate at which elevated cortisol drives the fractional suppression term $\gamma = \min(0.92, \max(0, \rho(C - 1)))$ in the disposal equation. This bounds the fractional suppression of glucose disposal within the physiologically plausible range $[0.0, 0.92]$, consistent with observed cortisol sensitivity in metabolic models [31]. This prevents divergence under extreme cortisol drive without altering the coupling structure. All simulations were integrated over a 7200-minute horizon (5 days) using the LSODA adaptive solver, sufficient to capture steady-state glucose equilibration under sustained stress drive.

Beyond stability, we addressed the model's tendency to pull participants toward a single metabolic average. While traditional models often treat glucose effectiveness as a population-wide constant [3], recent minimal model analyses have demonstrated that insulin-independent glucose disposal is a dynamic parameter that varies significantly with BMI and glucose tolerance status [25]. By scaling E to the individual's fasting baseline, we account for this observed reduction in non-insulin-mediated clearance pathways, which is critical for maintaining stability across the UK Biobank's glycemic spectrum.

The implementation of individualized scaling is further supported by hierarchical modeling of glucose effectiveness across 497 subjects, which demonstrated that glucose effectiveness at zero insulin (GEZI) is reduced from 0.021 min^{-1} in healthy populations to 0.011 min^{-1} in T2D [17]. The previous frameworks established population-wide constants ($H_{ref} = 2000.0$ mg/dL/d, $E = 24.48$ d^{-1}) [31], but we implemented individualized scaling to capture UKB cohort heterogeneity. Using binary search, we established a healthy reference $E_{ref} = 56.30$, anchoring the attractor at the healthy cohort mean $G_{ref} = 86.5$ mg/dL. The higher value relative to the Yildirim baseline reflects the distinct metabolic profile of the UKB healthy cohort, whose reference BMI and fasting glucose are lower than those used in the original model calibration. Each participant i receives a personalized uptake rate E_i:

$$E_i = E_{ref} \times \left(\frac{G_{ref}}{G_{0,i}} \right)^{\alpha} \tag{4}$$

where $\alpha = 0.984$. Biologically, this encodes the well-established finding that peripheral glucose uptake capacity is impaired in insulin-resistant individuals [9], representing a shift in glucose effectiveness often overlooked in simplified models [3]. To prevent diabetic participants ($G_{0,i} > 126$ mg/dL) from crossing into

ICCS Camera Ready Version 2026
To cite this paper please use the final published version:
DOI: 10.1007/978-3-032-29912-3_33

the healthy attractor, E_i is capped at a floor of $\phi = 0.75 \cdot E_{ref}$ (consistent with clinical estimates of impaired glucose effectiveness in secondary β-cell failure [4]). Finally, hepatic glucose production (H) is scaled sub-linearly to reflect chronic upregulation of gluconeogenesis:

$$H_{bas,i} = H_{ref} \times \left(\frac{G_{0,i}}{G_{ref}} \right)^{0.3} \tag{5}$$

Parameter Sensitivity Analysis The selection of metabolic parameters for local sensitivity analysis was informed by the pleiotropic effects of cortisol on glucose-insulin homeostasis. Clinical evidence indicates that chronic HPA activation suppresses β-cell function even after adjusting for baseline insulin resistance [20], and that glucose effectiveness (E) varies significantly across phenotypic clusters and body mass indices [19]. Consequently, we identified six primary parameters representing the mechanistic intersections between endocrine signaling and metabolic flux: target insulin sensitivity (S_{target}), basal hepatic glucose production (H_{bas}), basal glucose uptake (E), the stress-insulin impact coefficient (k_c), the cortisol inhibition factor (γ), and the insulin clearance rate (k). While E and H_{bas} were included to evaluate our individualized scaling framework, γ was selected to assess the systemic impact of the stability refinements discussed in *Numerical Stability and Calibration* section above.

Each parameter was perturbed by $\pm 10\%$ from its calibrated value while maintaining all other variables constant. The simulation was re-run across the diabetic cohort to quantify the resulting shift in mean steady-state glucose. The results (Figure 3A) confirm that S_{target} exhibits the greatest total sensitivity, followed by a cluster comprising H_{bas}, E, and γ with comparable moderate effects. The insulin clearance rate (k) demonstrates an asymmetric response, with sensitivity concentrated in the upward perturbation direction. This matches clinical observations of highly variable insulin degradation rates in T2D populations, where clearance defects often exacerbate the hyperglycemic state [31]. These results provide mathematical confirmation that E and H_{bas} occupy the sensitive tier of the system required to drive the bimodal phenotypic separation observed in the UK Biobank data.

3 Results

Population Distribution and Density. We first examined the model's ability to generate the distinct glucose distributions observed in the clinical data (Figure 2C). The distribution is right-skewed, with the majority of mass concentrated near the healthy range and an extended upper tail reaching into the diabetic range, reflecting the combined healthy and diabetic cohorts within the pilot. The quartile spread is further illustrated in the violin plot (Figure 2D); the model also follows the overall trajectory of the clinical reference, capturing the spread of both cohorts without requiring phenotype-specific parameter adjustments.

ICCS Camera Ready Version 2026
To cite this paper please use the final published version:
DOI: 10.1007/978-3-032-29912-3_33

Statistical Parity and Quantile Analysis. To assess the fit across the entire population, we analyzed the Empirical Cumulative Distribution Function (ECDF) and a Quantile-Quantile (Q-Q) plot. The ECDF (Figure 2B) demonstrates clear bimodal step behavior in both the clinical and simulated populations. A distinct plateau is observed between the 100 mg/dL (IFG) and 126 mg/dL (Diabetes) thresholds, indicating a partitioning of the cohort into two primary metabolic attractors. While the clinical data exhibits a slightly more aggressive transition in the pre-diabetic range, the model successfully reproduces the variance compression in the healthy attractor and the extended high-glucose tail characteristic of the diabetic phenotype. The Q-Q plot in Figure 2A provides a direct comparison of the clinical and simulated quantiles. The data points follow a nearly linear path along the diagonal reference line. We observed a small divergence at the bottom-left of the plot, indicating that the clinical data has a slightly different distribution at the lower-middle glucose thresholds (130-140 mg/dL). However,

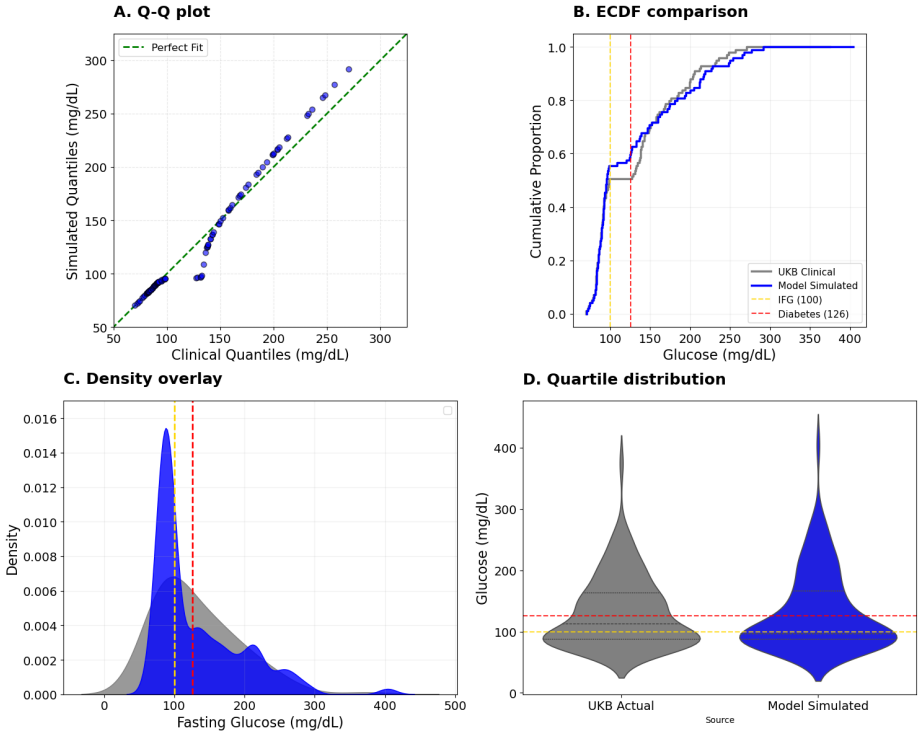

Fig. 2: Global statistical validation against the UK Biobank pilot cohort; the blue curve represents the model-simulated population and the grey shaded area the UK Biobank clinical reference. (A) Quantile-Quantile plot assessing distributional alignment. (B) ECDF comparison demonstrating cumulative parity and bimodal step behavior. (C) Population density overlay reproducing clinical metabolic hills. (D) Violin plot showing the simulated quartile distribution against clinical reference data.

ICCS Camera Ready Version 2026
To cite this paper please use the final published version:
DOI: 10.1007/978-3-032-29912-3_33

the overall linearity confirms that the model accurately captures the statistical variance and population-level distribution of the UK Biobank dataset.

Clinical Classification Accuracy. The model was evaluated on its ability to categorize participants into standard diagnostic bins: Normal (< 100 mg/dL), Impaired Fasting Glucose (IFG, $100 - 126$ mg/dL), and Diabetes (≥ 126 mg/dL). Figure 3C compares the diagnostic distribution between the clinical UK Biobank pilot cohort and the simulated results.

In the clinical dataset, the population is split evenly (50%) between the Normal and Diabetic categories. The simulated results show a slight shift in these proportions: 55% of participants were classified as Normal, 5% fell into the IFG range, and 40% reached the diabetic threshold. These results indicate that while the coupled HPA-metabolic framework captures the bimodal nature of the population, a subset of the diabetic cohort in the simulation transitioned toward lower glycemic categories. This suggests that the individualized scaling for insulin sensitivity and hepatic production separates the phenotypes, though it slightly underestimates the total diabetic count compared to the clinical reference.

The observed 5% shift from the diabetic to the IFG category in the simulation is primarily attributable to the deterministic behavior of the system near the G_{crit} boundary. Because the model relies on a single-attractor architecture for each individual, participants with baseline glucose levels just above the threshold may settle into a steady state slightly below 126 mg/dL depending on their specific HPA-metabolic coupling. This slight underestimation of the diabetic proportion reflects a limitation of the current deterministic framework rather than a deficiency in the individualized scaling logic, suggesting that the Impaired Fasting Glucose range in the model serves as a transitional buffer between healthy and diabetic metabolic states.

Mechanistic Emergence of Bimodality. Finally, we explored the structural behavior of the model through an alpha-sweep (Figure 3B). This visualization demonstrates how the population distribution evolves as the exponent governing individualized basal glucose uptake (α in Eq. 4) is increased from 0.1 toward the calibrated value of 0.984. At low α, all participants converge near the healthy attractor ($\sim$88 mg/dL), confirming the single-attractor problem of uncalibrated parameters. As α increases, the distribution progressively broadens rightward, with the diabetic cohort separating into a higher glycemic range, producing the right-skewed spread consistent with the UK Biobank data.

4 Discussion

The individualized calibration demonstrates that the Type 2 Diabetes transition can be modeled as a mechanistic shift in metabolic anchor points. Our results support the hypothesis that a coupled HPA-metabolic framework can maintain distinct phenotypic attractors through individualized scaling, reproducing clinical distributions without group-specific manual refitting. The power-law scaling

ICCS Camera Ready Version 2026
To cite this paper please use the final published version:
DOI: 10.1007/978-3-032-29912-3_33

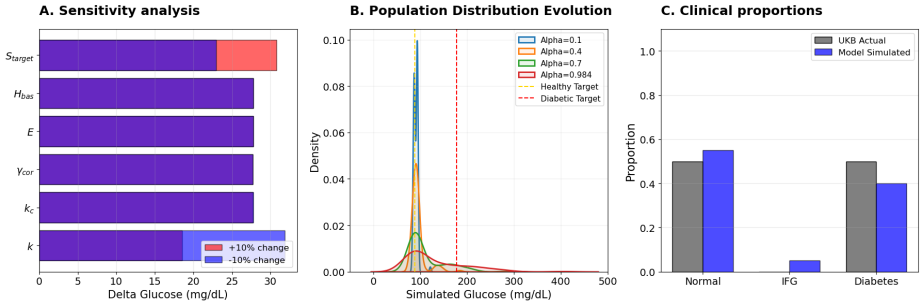

Fig. 3: Mechanistic insights and clinical verdict. (A) Tornado sensitivity analysis identifying primary drivers of the glucose steady state. (B) Alpha-sweep showing the mechanistic emergence of population bimodality. (C) Clinical proportions comparing simulated diagnostic categorization against the UK Biobank pilot.

for basal glucose uptake (E) and hepatic production (H) was necessary to prevent the healthy cohort from drifting toward a single population attractor, effectively capturing the metabolic heterogeneity of insulin-independent pathways [14]. This approach is underscored by the hierarchical modeling of Hu et al. [17], who identified that the contribution of insulin-independent disposal accounts for nearly 73% of whole-body clearance in healthy subjects, but collapses to approximately 49% in T2D. It is important to distinguish between the model's personalization capacity and its predictive scope. Because $G_{0,i}$ serves as the primary anchor for both E_i and $H_{bas,i}$, the distributional parity demonstrated in Section 3 confirms that the scaling logic is internally consistent but does not inherently constitute out-of-sample prediction. To address this potential circularity, we evaluated the simulated steady states against observed HbA1c (Field 30750), a marker of mean glycemic burden not used during initialization. The Pearson correlation between simulated 5-day steady-state glucose and observed HbA1c was $r = 0.82$ ($p < 0.0001$, $n = 95$). Within the diabetic cohort alone, $r = 0.69$ ($p < 0.0001$), while the negligible within-healthy correlation ($r = 0.04$, $p = 0.80$) is consistent with the narrow glycemic range of that cohort reducing available variance. These results indicate that the personalized steady states track an independent clinical marker of glycemic burden and are not merely a reflection of the initialization input.

ODE Attractors and Latent Trajectory Classes The emergence of bimodal hills in our simulated ECDF (Figure 2B) provides a mechanistic basis for the latent classes identified in recent longitudinal analyses of the UK Biobank. Using Latent Class Growth Mixture Modeling (LCGMM), Handley et al. identified six distinct HbA1c trajectory classes, where the dominant "low and stable" class (76.8%) represents the primary homeostatic attractor [1,16]. Our ODE framework offers a physiological explanation for this partitioning; by anchoring E_i to individual baselines, the system settles into distinct phenotypic manifolds rather than a single population average. The 5% shift from the diabetic to the IFG category in our simulation (Figure 3C) likely represents the "transitional" tra-

ICCS Camera Ready Version 2026
To cite this paper please use the final published version:
DOI: 10.1007/978-3-032-29912-3_33

jectories identified in parabolic latent classes, suggesting that metabolic drift is a continuous drift between stable metabolic regimes biased by mental health stressors [13].

Natural History vs. Managed Variance Compression A notable mismatch was observed in the standard deviation of the diabetic cohort (75.6 mg/dL in simulation vs 48 mg/dL in clinical data). Our model predicts higher glycemic extremes because it simulates an untreated natural history, whereas clinical snapshots in the UK Biobank reflect a "managed" state. This disparity illustrates the "variance compression" typical of Electronic Health Record (EHR) data; even though natural history models like Archimedes predict wide glycemic excursions in unmanaged states [12], real-world patients are stabilized by medication: within the UK Biobank diabetic cohort, approximately 66.3% of confirmed T2D participants at Instance 0 were recorded as receiving glucose-lowering agents (Field 20003), with metformin representing the dominant intervention. After applying our medication exclusion criteria, the untreated subsample used here therefore represents a self-selected minority whose natural disease trajectory is less attenuated than the broader clinical population. Specifically, interventions like Metformin truncate the upper tail of the distribution by aggressively suppressing the hepatic gluconeogenesis that our model identifies as a key driver of stress-induced hyperglycemia [28,22]. This clinical stabilization is further evidenced by the development of EHR-based risk assessments like the HypoHazardScore, which must account for this compressed clinical reality when translating trial-derived variability into practice [24].

Timescale Separation and Phenotypic Snapping The observed ambiguity in the IFG category suggests a limitation of the current deterministic framework - the lack of bistability needed to create a sharp threshold between healthy and diabetic states. This is likely due to the separation of timescales inherent in neuroendocrine regulation. While our five-day simulation captures fast dynamics of metabolic equilibration, actual transitions into disease states involve slower variable dynamics that evolve over months or years. Specifically, Karin et al. demonstrated that chronic stress induces gland mass hypertrophy in the pituitary and adrenal cortex, creating a structural "memory" that increases the system's gain over time [21]. Without these long-term morphological feedbacks, the model settles into transient equilibria rather than crossing into the irreversible basins of attraction identified in more complex HPA bifurcation analyses [30,2]. The 5-day simulation horizon used here is therefore best understood as capturing the fast equilibration dynamics of the glucose-insulin subsystem under a fixed stress drive, not as a direct model of the multi-year progression to T2D. Simulating the latter would require integrating the slow structural feedbacks (gland hypertrophy, β-cell exhaustion) that operate on timescales of months to years and are currently held constant in the state vector.

The Hyperglycemic Feed-forward Loop Our sensitivity analysis identified cortisol inhibition (γ) and insulin sensitivity (S_{target}) as the primary drivers of

ICCS Camera Ready Version 2026
To cite this paper please use the final published version:
DOI: 10.1007/978-3-032-29912-3_33

metabolic stability. This mathematical sensitivity reflects the "Noxious Ninth" hypothesis, in which HPA dysregulation functions as both cause and consequence of metabolic dysfunction [18]. Chronic hyperglycemia induces a state of "functional hypercortisolism" by elevating arginine vasopressin (AVP) levels, which synergizes with CRH to override the HPA axis "brakes" [7]. Mechanistically, the glucocorticoid-adiponectin axis acts as a key regulator of this drift, where elevated cortisol suppresses adiponectin expression via PPARγ antagonism, further driving metabolic instability [23]. By capturing this loop, our model illustrates how psychosocial stress and metabolic pressure form a self-reinforcing cycle that accelerates metabolic drift.

5 Conclusion

We have demonstrated that a coupled hypothalamic-pituitary-adrenal (HPA) and metabolic framework can be calibrated to high-dimensional clinical data by anchoring physiological parameters to a minimal set of individual markers. By transitioning from population-wide constants to individualized scaling for glucose effectiveness (E) and hepatic production (H), the model reproduced the bimodal glucose distributions observed in the UK Biobank pilot cohort without requiring group-specific refitting. Notably, this framework achieves clinical parity using only two primary inputs from the UK Biobank: baseline fasting glucose and mental health symptom burden. While other physiological parameters currently remain static or scaled to these anchors, the model's ability to maintain distinct phenotypic attractors proves that this low-input approach is sufficient to capture the emergent metabolic drift of the population. The correlation between simulated glucose and independently observed HbA1c ($r = 0.82$, $p < 0.0001$) further supports that the framework captures clinically meaningful signal beyond the initialization anchor.

The success of this pilot confirms that the framework is suitable for scaling to the full UK Biobank population to identify potential targets for clinical decision-making. However, the observed ambiguity in the pre-diabetic/IFG range highlights the necessity of longer-term simulations that account for slow-moving structural feedbacks, such as gland mass hypertrophy and β-cell exhaustion, which determine the irreversible basins of attraction for metabolic disease [21].

This study constitutes the first stage of a broader research programme aimed at building a population-scale neuroendocrine-metabolic model for the UK Biobank. The immediate next step is extending the individualized scaling framework to a larger cohort while incorporating additional interacting systems (including CNS-HPA feedbacks and longitudinal weight dynamics) validated against the UK Biobank. Longer-term, Neural ODE and DeepONet architectures are being explored to capture the high-dimensional trajectory dynamics that deterministic ODE systems approximate at the population level. The pilot results presented here confirm that the mechanistic foundation is sound and the scaling approach is viable, establishing the basis for virtual stress-reduction trials at scale.

ICCS Camera Ready Version 2026
To cite this paper please use the final published version:
DOI: 10.1007/978-3-032-29912-3_33

Data Availability Statement. The code and synthetic data necessary to reproduce the mechanistic simulations in this study are publicly available on GitHub at https://github.com/rezi-getsadze/HPA-Metabolic-UKB and permanently archived at https://doi.org/10.5281/zenodo.19431079. The clinical validation data were obtained from the UK Biobank. Because the UK Biobank contains sensitive human health and biometric data, the individual-level participant data cannot be shared publicly by the authors. Researchers can apply for access to this data directly through the UK Biobank management system.

Acknowledgments. This research and the acquisition of the UK Biobank dataset were supported by a seed grant from the University of Amsterdam (UvA) Research Priority Area Personal Microbiome Health (RPA-PMH) under the project 'DIGEST'. The authors also acknowledge SURF for funding the computational resources utilized in this study.

Disclosure of Interests. The authors have no competing interests to declare that are relevant to the content of this article.

A Modified ODE Equations

The full 18-equation HPA-metabolic system is defined in Cao et al. [6], drawing on Karin et al. [21] for the HPA axis module and Yildirim et al. [31] for the metabolic module. We reproduce here only the equations substantively modified in this work.

The glucocorticoid feedback factor g_C and stress drive u are:

$$g_C = \frac{1}{1 + (C/k_{gr})^n}, \qquad u = u_{min} + (S \cdot \Delta u) \tag{6}$$

Glucose dynamics are governed by $\frac{dG}{dt} = H(C, G) - R(C, G, I)$, where:

$$H = H_{bas} + \frac{(1 + c_h(C - 1)) \cdot H_{max} \cdot k_h^{n_h}}{k_h^{n_h} + (s^{hep} \cdot I)^{n_h}} \tag{7}$$

$$R = \left(E + c_s \cdot s \cdot I + \frac{(1 - \gamma') \cdot R_{max} \cdot (sI)^{n_R}}{(1 - \gamma) \cdot k_R^{n_R} + (sI)^{n_R}} \right) G \tag{8}$$

where $\gamma = \min(0.92, \max(0, \rho(C - 1)))$ with $\rho = 0.08$ (reduced from the Cao et al. default to ensure numerical stability across the UK Biobank glycemic range), and $\gamma' = \min(0.92, \max(0, \rho'(C - 1)))$. The individualized parameters E_i and $H_{bas,i}$ are defined in Eqs. 4-5 of the main text. All remaining state equations (insulin dynamics, FFA, insulin sensitivity, beta-cell mass, inflammation, body weight, fat compartments) follow Cao et al. [6] without modification.

ICCS Camera Ready Version 2026
To cite this paper please use the final published version:
DOI: 10.1007/978-3-032-29912-3_33

References

1. Ahlqvist, E., Storm, P., Käräjämäki, A., Martinell, M., Dorkhan, M., Carlsson, A., Vikman, P., Prasad, R.B., Aly, D.M., Almgren, P., Wessman, Y., Shaat, N., Spégel, P., Mulder, H., Lindholm, E., Melander, O., Hansson, O., Malmqvist, U., Lernmark, Å., Lahti, K., Forsén, T., Tuomi, T., Rosengren, A.H., Groop, L.: Novel subgroups of adult-onset diabetes and their association with outcomes: a data-driven cluster analysis of six variables. The Lancet Diabetes & Endocrinology **6**(5), 361–369 (May 2018). https://doi.org/10.1016/S2213-8587(18)30051-2
2. Andersen, M., Vinther, F., Ottesen, J.T.: Mathematical modeling of the hypothalamic–pituitary–adrenal gland (HPA) axis, including hippocampal mechanisms. Mathematical Biosciences **246**(1), 122–138 (Nov 2013). https://doi.org/10.1016/j.mbs.2013.08.010
3. Bergman, R.N., Ider, Y.Z., Bowden, C.R., Cobelli, C.: Quantitative estimation of insulin sensitivity. American Journal of Physiology-Endocrinology and Metabolism **236**(6), E667 (1979). https://doi.org/10.1152/ajpendo.1979.236.6.E667, https://doi.org/10.1152/ajpendo.1979.236.6.E667
4. Best, J.D., Kahn, S.E., Ader, M., Watanabe, R.M., Ni, T.C., Bergman, R.N.: Role of Glucose Effectiveness in the Determination of Glucose Tolerance. Diabetes Care **19**(9), 1018–1030 (Sep 1996). https://doi.org/10.2337/diacare.19.9.1018
5. Bumbuc, R., Yildirim, V., Sheraton, M.: Modelling the Interplay Between Chronic Stress and Type 2 Diabetes On-Set. In: Computational Science – ICCS 2023 (Jun 2023). https://doi.org/10.1007/978-3-031-36021-3_34
6. Cao, Q., Yildirim, V., Nicolaou, M., Sheraton, V.M.: A Human Cohort Data Validated Mechanistic Model Linking Psychosocial Stress to Type 2 Diabetes Risk (Mar 2026). https://doi.org/10.21203/rs.3.rs-9260829/v1, https://www.researchsquare.com/article/rs-9260829/v1, iSSN: 2693-5015
7. Champaneri, S., Xu, X., Carnethon, M.R., Bertoni, A.G., Seeman, T., Diez Roux, A., Golden, S.H.: Diurnal salivary cortisol and urinary catecholamines are associated with diabetes mellitus: the Multi-Ethnic Study of Atherosclerosis. Metabolism: Clinical and Experimental **61**(7), 986–995 (Jul 2012). https://doi.org/10.1016/j.metabol.2011.11.006
8. Chrousos, G.P.: Stress and disorders of the stress system. Nature Reviews Endocrinology **5**(7), 374–381 (Jul 2009). https://doi.org/10.1038/nrendo.2009.106
9. DeFronzo, R.A.: The Triumvirate: β-Cell, Muscle, Liver: A Collusion responsible for NIDDM. Diabetes **37**(6), 667–687 (Jun 1988). https://doi.org/10.2337/diab.37.6.667
10. Dias, J.P., Joseph, J.J., Kluwe, B., Zhao, S., Shardell, M., Seeman, T., Needham, B.L., Wand, G.S., Kline, D., Brock, G., Castro-Diehl, C., Golden, S.H.: The longitudinal association of changes in diurnal cortisol features with fasting glucose: MESA. Psychoneuroendocrinology **119**, 104698 (Sep 2020). https://doi.org/10.1016/j.psyneuen.2020.104698
11. Ditmars, H.L., Logue, M.W., Toomey, R., McKenzie, R.E., Franz, C.E., Panizzon, M.S., Reynolds, C.A., Cuthbert, K.N., Vandiver, R., Gustavson, D.E., Eglit, G.M.L., Elman, J.A., Sanderson-Cimino, M., Williams, M.E., Andreassen, O.A., Dale, A.M., Eyler, L.T., Fennema-Notestine, C., Gillespie, N.A., Hauger, R.L., Jak, A.J., Neale, M.C., Tu, X.M., Whitsel, N., Xian, H., Kremen, W.S., Lyons, M.J.: Associations between depression and cardiometabolic health: A 27-year longitudinal study. Psychological Medicine **52**(14), 3007–3017 (Oct 2022). https://doi.org/10.1017/S003329172000505X

ICCS Camera Ready Version 2026
To cite this paper please use the final published version:
DOI: 10.1007/978-3-032-29912-3_33

12. Eddy, D.M., Schlessinger, L.: Archimedes: a trial-validated model of diabetes. Diabetes Care **26**(11), 3093–3101 (Nov 2003). https://doi.org/10.2337/diacare.26.11.3093
13. Gillett, A., Handley, D., Bala, R., Young, K., Tyrrell, J., Lewis, C.: Impact of depression on treatment progression in type 2 diabetes: A UK retrospective cohort study using the Clinical Practice Research Datalink Aurum databas (2025). https://doi.org/10.1101/2025.11.19.25340563
14. Ha, J., Sherman, A.: Type 2 diabetes: one disease, many pathways. American Journal of Physiology-Endocrinology and Metabolism **319**(2), E410–E426 (2020). https://doi.org/10.1152/ajpendo.00512.2019, https://doi.org/10.1152/ajpendo.00512.2019
15. Hackett, R.A., Kivimäki, M., Kumari, M., Steptoe, A.: Diurnal Cortisol Patterns, Future Diabetes, and Impaired Glucose Metabolism in the Whitehall II Cohort Study. The Journal of Clinical Endocrinology & Metabolism **101**(2), 619–625 (Feb 2016). https://doi.org/10.1210/jc.2015-2853
16. Handley, D., Gillett, A.C., Bala, R., Tyrrell, J., Lewis, C.M.: Latent class growth mixture modeling of HbA1C trajectories identifies individuals at high risk of developing complications of type 2 diabetes mellitus in the UK Biobank. BMJ Open Diabetes Research & Care **13**(5) (Sep 2025). https://doi.org/10.1136/bmjdrc-2024-004826
17. Hu, S., Lu, Y., Tura, A., Pacini, G., D'Argenio, D.Z.: An Analysis of Glucose Effectiveness in Subjects With or Without Type 2 Diabetes via Hierarchical Modeling. Frontiers in Endocrinology **12** (Mar 2021). https://doi.org/10.3389/fendo.2021.641713
18. Isidori, A.M., Pofi, R., Fleseriu, M.: Beyond the Classical Axis: Metabolic "Pressure" on the Adrenal Gland? Diabetes **74**(12), 2207–2210 (Nov 2025). https://doi.org/10.2337/dbi25-0035
19. Kahn, S.E., Prigeon, R.L., McCulloch, D.K., Boyko, E.J., Bergman, R.N., Schwartz, M.W., Neifing, J.L., Ward, W.K., Beard, J.C., Palmer, Jr, J.P.: The Contribution of Insulin-Dependent and Insulin-Independent Glucose Uptake to Intravenous Glucose Tolerance in Healthy Human Subjects. Diabetes **43**(4), 587–592 (Apr 1994). https://doi.org/10.2337/diab.43.4.587
20. Kamba, A., Daimon, M., Murakami, H., Otaka, H., Matsuki, K., Sato, E., Tanabe, J., Takayasu, S., Matsuhashi, Y., Yanagimachi, M., Terui, K., Kageyama, K., Tokuda, I., Takahashi, I., Nakaji, S.: Association between Higher Serum Cortisol Levels and Decreased Insulin Secretion in a General Population. PLOS ONE **11**(11), e0166077 (Nov 2016). https://doi.org/10.1371/journal.pone.0166077
21. Karin, O., Raz, M., Tendler, A., Bar, A., Korem Kohanim, Y., Milo, T., Alon, U.: A new model for the HPA axis explains dysregulation of stress hormones on the timescale of weeks. Molecular Systems Biology **16**(7), MSB209510 (Jul 2020). https://doi.org/10.15252/msb.20209510
22. Khani, S., Tayek, J.A.: Cortisol increases gluconeogenesis in humans: its role in the metabolic syndrome. Clinical Science **101**(6), 739–747 (Nov 2001). https://doi.org/10.1042/cs1010739
23. Luo, L., Wang, L., Luo, Y., Romero, E., Yang, X., Liu, M.: Glucocorticoid/Adiponectin Axis Mediates Full Activation of Cold-Induced Beige Fat Thermogenesis. Biomolecules **11**(11), 1573 (Oct 2021). https://doi.org/10.3390/biom11111573
24. Ma, S., Alvear, A., Schreiner, P.J., Seaquist, E.R., Kirsh, T., Chow, L.S.: Development and Validation of an Electronic Health Record-Based Risk Assessment Tool

ICCS Camera Ready Version 2026
To cite this paper please use the final published version:
DOI: 10.1007/978-3-032-29912-3_33

for Hypoglycemia in Patients With Type 2 Diabetes Mellitus. Journal of Diabetes Science and Technology **19**(1), 105–113 (Jan 2025). https://doi.org/10.1177/19322968231184497

25. Morettini, M., Di Nardo, F., Ingrillini, L., Fioretti, S., Göbl, C., Kautzky-Willer, A., Tura, A., Pacini, G., Burattini, L.: Glucose effectiveness and its components in relation to body mass index. European Journal of Clinical Investigation **49**(6), e13099 (2019). https://doi.org/10.1111/eci.13099, https://onlinelibrary.wiley.com/doi/pdf/10.1111/eci.13099
26. Pan, A., Lucas, M., Sun, Q., van Dam, R.M., Franco, O.H., Manson, J.E., Willett, W.C., Ascherio, A., Hu, F.B.: Bidirectional Association Between Depression and Type 2 Diabetes Mellitus in Women. Archives of Internal Medicine **170**(21), 1884–1891 (Nov 2010). https://doi.org/10.1001/archinternmed.2010.356
27. Rizza, R.A., Mandarino, L.J., Gerich, J.E.: Cortisol-Induced Insulin Resistance in Man: Impaired Suppression of Glucose Production and Stimulation of Glucose Utilization due to a Postreceptor Defect of Insulin Action*. The Journal of Clinical Endocrinology & Metabolism **54**(1), 131–138 (Jan 1982). https://doi.org/10.1210/jcem-54-1-131
28. Stern, M., Williams, K., Eddy, D., Kahn, R.: Validation of prediction of diabetes by the Archimedes model and comparison with other predicting models. Diabetes Care **31**(8), 1670–1671 (Aug 2008). https://doi.org/10.2337/dc08-0521
29. Sudlow, C., Gallacher, J., Allen, N., Beral, V., Burton, P., Danesh, J., Downey, P., Elliott, P., Green, J., Landray, M., Liu, B., Matthews, P., Ong, G., Pell, J., Silman, A., Young, A., Sprosen, T., Peakman, T., Collins, R.: UK Biobank: An Open Access Resource for Identifying the Causes of a Wide Range of Complex Diseases of Middle and Old Age. PLOS Medicine **12**(3), e1001779 (Mar 2015). https://doi.org/10.1371/journal.pmed.1001779
30. Weir, G.C., Bonner-Weir, S.: Five stages of evolving beta-cell dysfunction during progression to diabetes. Diabetes **53 Suppl 3**, S16–21 (Dec 2004). https://doi.org/10.2337/diabetes.53.suppl_3.s16
31. Yildirim, V., Sheraton, V.M., Brands, R., Crielaard, L., Quax, R., Riel, N.A.W.v., Stronks, K., Nicolaou, M., Sloot, P.M.A.: A data-driven computational model for obesity-driven diabetes onset and remission through weight loss. iScience **26**(11) (Nov 2023). https://doi.org/10.1016/j.isci.2023.108324

ICCS Camera Ready Version 2026
To cite this paper please use the final published version:
DOI: 10.1007/978-3-032-29912-3_33